REVIEW

Atomic resolution structure determination by the cryo-EM method MicroED

Shian Liu, Johan Hattne, Francis E. Reyes, Silvia Sanchez-Martinez, M. Jason de la Cruz, Dan Shi, and Tamir Gonen*

Janelia Research Campus, Howard Hughes Medical Institute, 19700 Helix Drive, Ashburn, Virginia 20148

Received 20 May 2016; Accepted 19 July 2016
DOI: 10.1002/pro.2989
Published online 25 July 2016 proteinscience.org

Abstract: The electron cryo-microscopy (cryoEM) method MicroED has been rapidly developing. In this review we highlight some of the key steps in MicroED from crystal analysis to structure determination. We compare and contrast MicroED and the latest X-ray based diffraction method the X-ray free-electron laser (XFEL). Strengths and shortcomings of both MicroED and XFEL are discussed. Finally, all current MicroED structures are tabulated with a view to the future.

Keywords: cryo EM; MicroED; crystallography; nano crystals

Introduction

Structural biologists use various methods to reveal inter- and intra-molecular interactions to understand the complicated chemical and physical processes of life. The pursuit of visualizing such detailed interactions has predominately relied on X-ray crystallography. However, cryo-electron microscopy (cryo-EM) has in recent years gained incredible momentum with ground-breaking advances in detector technology[1] and the development of new methodologies.[2]

Modern cryo-EM diversified into four methods: tomography, single-particle reconstructions, two-dimensional (2D) electron crystallography and MicroED (Fig. 1). Cryo-electron tomography was developed to study whole cells and large organelles albeit at relatively modest resolutions of ~1 nm.[7,8] In single-particle reconstructions imaging thousands of isolated and purified particles in vitrified ice followed by motion correction, averaging and reconstruction can yield structures close to 2Å in resolution for well-behaved samples.[4,9] The last two methods in cryo-EM rely on having crystalline material. Electron crystallography can use imaging and/or diffraction from highly ordered 2D crystals to obtain structures of membrane proteins embedded in a lipid bilayer. This method has yielded the structure of the water channel aquaporin-0 and its surrounding membrane at 1.9 Å resolution from 2D crystals only a single protein layer thick.[5,10] Finally, in MicroED vanishingly small three-dimensional (3D) crystals of biological material are studied by electron diffraction under cryogenic conditions to reveal unprecedented atomic detail such as the positions of protons in a protein.[6,11] In this review, we highlight the unique strengths of MicroED and summarize current advances in this method.

Brief Overview of MicroED

As with any crystallography experiments, MicroED relies on having well-ordered crystals. The same

Abbreviations: CMOS,, complementary metal-oxide semiconductor; cryo-EM,, cryo-electron microscopy; SFX,, Serial femtosecond crystallography; XFEL,, X-ray free-electron laser

Grant sponsor: Howard Hughes Medical Institute (to Gonen laboratory).

*Correspondence to: T. Gonen, Janelia Research Campus, Howard Hughes Medical Institute, 19700 Helix Drive, Ashburn, VA 20148. E-mail: gonent@janelia.hhm.org

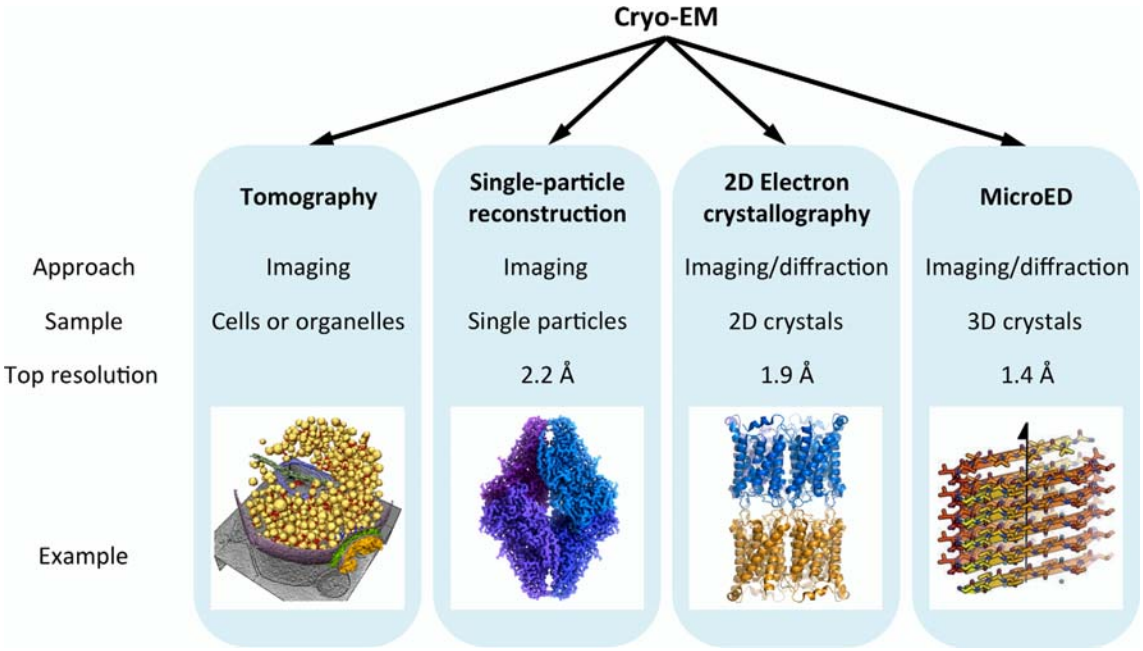

Figure 1. Four methods in Cryo EM. From left to right, a synaptosome model (reprinted from Ref. 3), a 2.2 Å structural model of β-galactosidase (reprinted from EMDB-2984 entry webpage[4]), the 1.9 Å resolution model of aquaporin-0,[5] and a 1.4 Å structural model of the α-synuclein NACore stacked in 3D space.[6]

crystallization robots and setups are used to screen for crystal growth as in X-ray crystallography. However, crystals for MicroED are typically billions of times smaller in volume than those used for X-ray crystallography. A discussion of how to find such small crystals in the crystallization drops was recently published along with a detailed protocol for data collection and processing.[12,13] Once crystals are identified in the crystallization drops (either by negative stain EM, optical means or powder diffraction) they are placed on an EM grid, plunged into liquid ethane for freezing and viewed in a cryo-electron microscope.

The examination in cryo applies three different dose rates sequentially. An initial grid screening at an ultra low dose rate ($< 10^{-6}$ e^- $Å^{-2}$ s^{-1}) with low magnification in bright field is performed to survey for thin crystals. Next, the microscope is switched to over-focused diffraction mode at $< 10^{-3}$ e^- $Å^{-2}$ s^{-1}, where each crystal is inspected individually. If a crystal shows appreciable diffraction, a final dose rate of 0.01-0.05 e^- $Å^{-2}$ s^{-1} is applied to collect the MicroED data set.

During data collection, crystals can be either tilted discretely or rotated continuously in the electron beam (Fig. 2). The initial MicroED data were collected as a series of still exposures, each of which captured one diffraction pattern at a certain discrete angle.[2] As the stage was tilted each time with an increment of 0.1-1°, a complete dataset of up to 90° worth of patterns per crystal were collected for determining the structure of lysozyme. With such experimental setup all reflections are only partially recorded, which hampers scaling and merging. This issue was solved by an improved data collection scheme for MicroED called continuous rotation.[12,14] This improved method yields data where reflections are fully recorded over a contiguous sequence of images, as diffraction occurs continuously while the crystal is rotating in the electron beam and the data is recorded as a movie on a fast complementary metal-oxide semiconductor (CMOS)-based detector.[12]

Data processing has also improved since the initial proof-of-principle study. Initial still diffraction data was processed using an in-house developed program specifically designed for lysozyme.[15] However, with continuous rotation each frame of the movie contains a wedge of data, typically between 0.1-0.5°, which is analogous to images collected using the rotation method in X-ray crystallography.[16] As such, continuous rotation MicroED data can be processed using standard X-ray crystallography data reduction software[17] such as MOSFLM[18,19] and XDS.[20] Detailed guidelines on data processing can be found in reference.[13]

Comparisons Between MicroED and XFEL

The ratio of inelastic to elastic scattering in an X-ray experiment is high in comparison with electrons; and X-rays deposit more destructive energy onto the sample.[21] Therefore, in traditional X-ray crystallography very large crystals are needed to

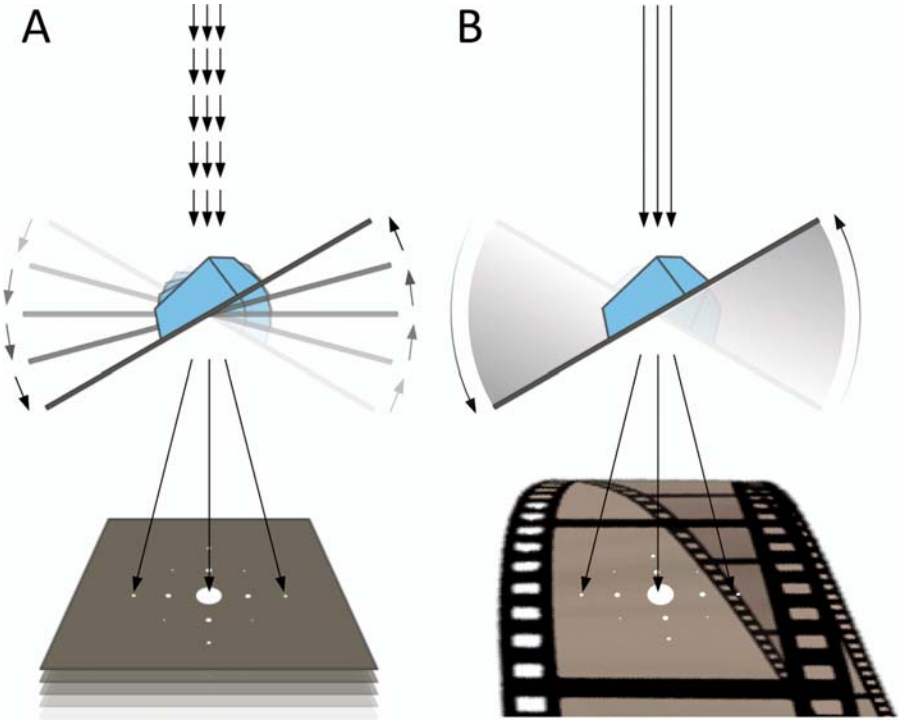

Figure 2. Illustration of two data collection approaches in MicroED. **A**. Still diffraction strategy where the beam gives a pulse of electrons and the crystal is rotated stepwise between exposures. **B.** Continuous rotation MicroED where the beam is constantly on, the crystal is rotating continuously in the diffracting beam and the data is recorded as in a movie on the fast camera. (The film in the figure is adapted from "Thondon entertainment" by Jathurchan, CCBY-SA3.0).

obtain interpretable diffraction patterns and to withstand the large radiation dose that accumulates during the collection of a complete rotation series from a single crystal.[22] Newly developed technologies use a more intense and short X-ray pulse to allow data collection from smaller crystals. Data sets are then obtained by merging the intensities integrated on thousands of diffraction patterns originating from millions of crystals.[23]

Serial femtosecond crystallography (SFX) at an X-ray free-electron laser (XFEL) can provide high-resolution diffraction data from small crystals. The high intensity beam obliterates the crystal after one exposure, but before the crystal is destroyed diffraction is collected.[24] This so-called "diffract before destroy" has become increasingly popular and a number of structures have already been determined by this diffraction method.[23,25–32] Of course those were facilitated by large instrument development[33–35] and software development for data reduction.[36–39] The main strengths of an XFEL experiment are that crystals can be smaller than the usual crystals used for traditional X-ray crystallography at home sources or synchrotrons[23] and that time resolved studies of dynamical processes could be conducted.[40–42] The shortcomings are that the cost of the experiment is prohibitively high, instrument beam time availability is very low, and difficulties processing the large amount of data that is rapidly produced. Furthermore, recent studies indicate that even SFX data is affected by radiation damage.[43] Since the pulse is too short for the crystal to rotate during the exposure each crystal only provides one still diffraction pattern before it is destroyed, and the reflections that are collected are always partially recorded leading to problems with scaling. Further complications arise from the variance in the exposed crystal volume in each shot, and fluctuations in the pulse intensity. Scaling is achieved by merging the reflections originating from thousands of diffraction patterns.[44,45] Finally, sample delivery is commonly achieved via a nozzle that sprays grams of crystalline material at the diffracting beam, therefore the sample requirement is high and the delivery nozzle can quite frequently clog up stopping the experiments.[46–48]

MicroED promises to overcome many of the obstacles encountered by an XFEL while maintaining many of the strengths and benefits. The quantity of crystalline material in a MicroED experiment can be much smaller than in an XFEL experiment. The smallest crystals used successfully were of a fragment of α-synuclein. The structure was determined at 1.4 Å resolution from crystals that were only ~50 nm thick.[6] With careful data collection and analysis, structures with very limited beam damage

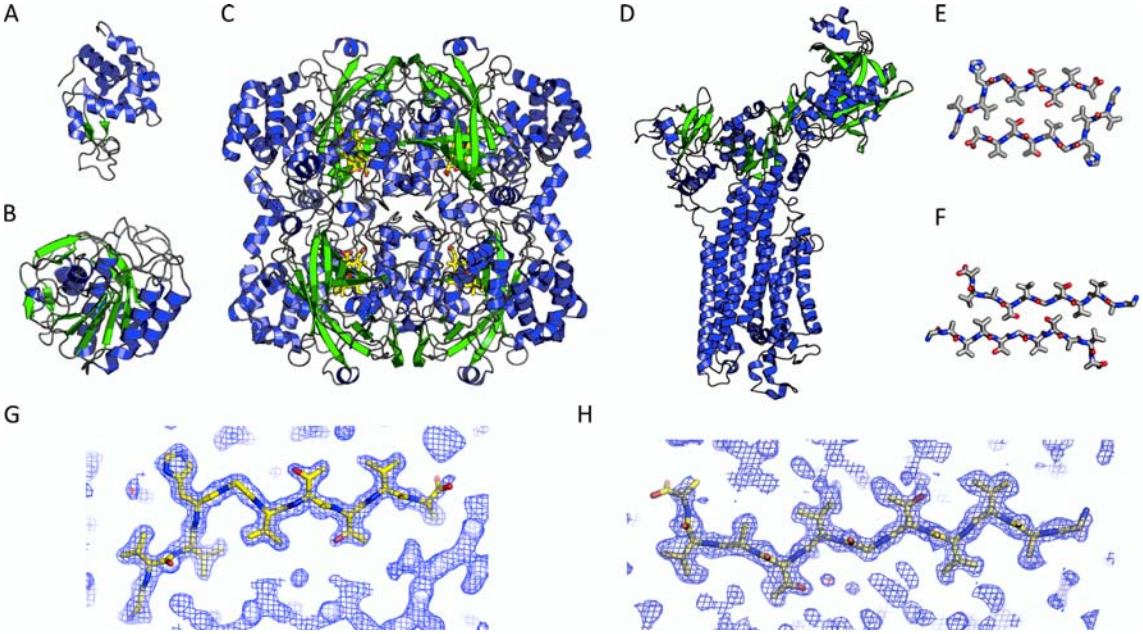

Figure 3. Structures of a few MicroED strcutrues. Cartoon representation of protein structures determined in MicroED, (A) lysozyme, (B) proteinase K, (C) catalase, (D) Ca^{2+}-ATPase, (E) α-synuclein preNAC and (F) NACore. The 2Fo-Fc electron density maps overlaid with structural models of E and F are shown in G and H, respectively.

can be determined from diffraction patterns of radiation-sensitive biological material recorded using very low electron dose (down to 10^{-6} $e^{-}/Å^2/s$) under cryogenic conditions.[14] The equipment needed for a MicroED experiment is relatively cheap and readily available, and no modifications are necessary to the electron microscope.[12] Time resolved and dynamic studies of biological systems can likewise be achieved as activators and inhibitors, pH or light can be used to start or stop a chemical reaction in the crystals right before plunge freezing into ethane and data collection. Such studies have already been conducted by electron crystallography of 2D crystals decades ago.[49,50] A single nanocrystal is sufficient for an entire data set to be collected and determined by MicroED.[14,17] Here the data is collected by continuous rotation, so full reflections are recorded, and data analysis can be done using standard crystallographic software like MOSFLM[19] and XDS[20] without modifications to the data reduction software.[14] Data collection and data analysis take ~10 minutes, respectively, followed by standard structure refinement. Finally, the highest resolution achieved by MicroED so far surpasses what was achieved in XFEL as well as any other cryo-EM method.

Some of the possible shortcomings in MicroED are shared with any crystal-based methods. MicroED depends on having well ordered crystals. If such crystals cannot grow then no crystallographic based method can be applied for structure solution. It is currently unclear what is the largest asymmetric unit that can be investigated by MicroED. To date the largest reported was that of catalase where two catalase proteins occupied the asymmetric unit amassing at ~500 kDa.[17] It is possible that for even larger asymmetric unit cells, large detector chips should be used to allow sufficient separation between diffraction spots for effective indexing. Better sample preparation methods are necessary for MicroED. The current cryo grid preparation methods that are blotting based can damage delicate crystals and the water–air interface that is created

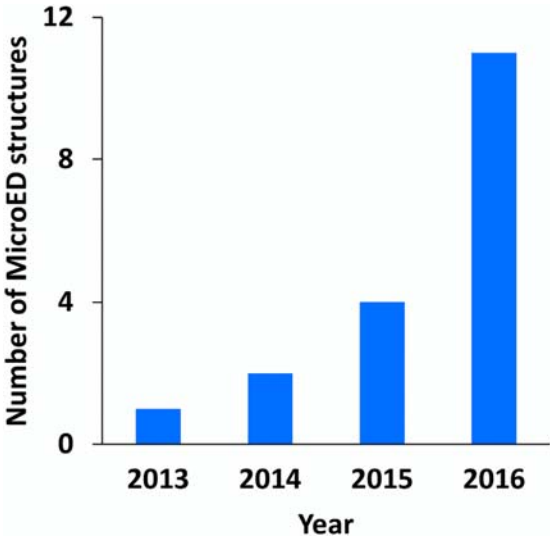

Figure 4. Number of MicroED structures determined since the first paper in 2013 to today.

Table I. *Summary of MicroED Structures From 2013 to 2016*

	Year	Data collection approach	Resolution	PDB	EMDB	SBGRID
Lysozyme	2013	Still diffraction	2.9 Å	3J4G[2]	2945	
	2014	Continuous rotation	2.5 Å	3J6K[14]	6342	185
	2016	Continuous rotation	1.5 Å	5K7O	8217	
Catalase	2014	Continuous rotation	3.2 Å	3J7B[17]	6314	186
	2015	Continuous rotation	3.2 Å	3J7U[51]		
Ca^{2+}-ATPase	2015	Continuous rotation	3.4 Å	3J7T[51]		
α-synuclein NACore	2015	Continuous rotation	1.4 Å	4RIL[6]	3028	193
α-synuclein preNAC	2015	Continuous rotation	1.4 Å	4ZNN[6]	3001	
Proteinase K	2016	Continuous rotation	1.75 Å	5I9S[52]	8077	262
	2016	Continuous rotation	1.3 Å	5K7S	8221	
Prion Zn-NNQQNY	2016	Continuous rotation	1.0 Å	5K2E[11]	8196	
Prion Cd-NNQQNY	2016	Continuous rotation	1.0 Å	5K2F[11]	8197	
Prion GNNQQNY1	2016	Continuous rotation	1.1 Å	5K2G[11]	8198	
Prion GNNQQNY2	2016	Continuous rotation	1.05 Å	5K2H[11]	8199	
Tau peptide	2016	Continuous rotation	1.1 Å	5K7N	8216	
Xylanase	2016	Continuous rotation	1.9 Å	5K7P	8218	
Thaumatin	2016	Continuous rotation	2.11 Å	5K7Q	8219	
Trypsin	2016	Continuous rotation	1.5 Å	5K7R	8220	
Thermolysin	2016	Continuous rotation	1.6 Å	5K7T	8222	

can likewise cause proteins to unwind and aggregate. Injection or laminar flow sample delivery methods should be developed to eliminate this issue and to increase the throughput of crystal screening.

Examples

Several protein structures have been determined by MicroED so far (Fig. 3). Those are summarized in Table I and Figure 4. The first structure solved was that of lysozyme at 2.9 Å resolution by still diffraction[2] and then at 2.5 Å resolution by continuous rotation.[14] This was followed by the 3.2 Å resolution structure of catalase, which was determined from a single nanocrystal only 8 protein layers thick,[17,51] and Ca^{2+}/ATPase.[51]

In late 2015 the first novel structures determined by MicroED were published.[6] Fragments of the toxic core of α-synuclein were determined at 1.4 Å resolution. Previous studies have shown that α-synuclein is the main component of neuron-associated aggregates or Lewy bodies that cause neurodegenerative diseases such as Parkinson disease. The formation of these aggregates relies on an 11-residue segment of α-synuclein, termed NACore. These NACore crystals, which were smaller than the wavelength of light, were in fact invisible in light microscopy, and the structure determined from 50 nm thick crystals. Such small crystals were not suitable for any X-ray based diffraction studies including XFEL, but they did yield a high-resolution structure by MicroED where H-atoms were observed for the first time by cryo-EM (Fig. 3). A close inspection of the NACore structure revealed that the twist of the β-sheets creates a tension for the protofilament of amyloid aggregates, which likely restrains the growth of the crystals. This new structural information shed light upon amyloid nucleation and could have implications for treatment of neurodegenerative diseases through inhibitor design strategies.

Recently the structures of four prion peptides were determined at 1 Å resolution by MicroED and direct phasing methods.[11] Prior to these examples, all other MicroED structures were phased by molecular replacement, where phases from a previously determined structure are applied to the measured structure factor amplitudes and refined to provide a new solution.[53] However, when the resolution obtained is high enough direct methods can be used for solving the phase problem.[54] This *ab initio* approach to phasing relies on the relationship between structure factors in reciprocal space, as well as constraints in real space.[54] This method requires very accurate measurements of the diffracted intensities at high resolution, typically around 1 Å. The fact that four structures could be determined by such methods from MicroED data indicates that the intensities collected in a continuous rotation MicroED experiment are very accurate and do not suffer from dynamical artifacts as previously wrongly suggested by others.[55]

Future Direction

As MicroED matures additional structures will be solved and provide new biological insights from crystals that are vanishingly small. Future developments in the method should focus on phasing and sample delivery. While molecular replacement is powerful, other phasing methods must be employed if no search model is available. Direct phasing can be done if the resolution obtained is close to 1 Å. Otherwise phasing by isomorphous methods using heavy metals may be a viable option. Phasing by imaging crystals can also be achieved or by using low-resolution density maps obtained by single

particle methods. Sample delivery needs to be improved and may include electro spray or capillary based methods in the future. Electron scattering factors need to be optimized to account for the scattering observed in a MicroED experiment and the entire method should be automated from data collection to structure determination. With such advances we expect a bright future for MicroED in the structural biology community.

Acknowledgments

The authors thank all of our collaborators and support staff and facilities at Janelia and beyond.

References

1. Faruqi AR, Henderson R (2007) Electronic detectors for electron microscopy. Curr Opin Struct Biol 17:549–555.
2. Shi D, Nannenga BL, Iadanza MG, Gonen T (2013) Three-dimensional electron crystallography of protein microcrystals. Elife 2:e01345.
3. Subramanian G, Basu S, Liu H, Zuo JM, Spence JC (2015) Solving protein nanocrystals by cryo-EM diffraction: multiple scattering artifacts. Ultramicroscopy 148: 87–93.
4. Bartesaghi A, Merk A, Banerjee S, Matthies D, Wu X, Milne JL, Subramaniam S (2015) 2.2 A resolution cryo-EM structure of beta-galactosidase in complex with a cell-permeant inhibitor. Science 348:1147–1151.
5. Gonen T, Cheng Y, Sliz P, Hiroaki Y, Fujiyoshi Y, Harrison SC, Walz T (2005) Lipid-protein interactions in double-layered two-dimensional AQP0 crystals. Nature 438:633–638.
6. Rodriguez JA, Ivanova MI, Sawaya MR, Cascio D, Reyes FE, Shi D, Sangwan S, Guenther EL, Johnson LM, Zhang M, Jiang L, Arbing MA, Nannenga BL, Hattne J, Whitelegge J, Brewster AS, Messerschmidt M, Boutet S, Sauter NK, Gonen T, Eisenberg DS (2015) Structure of the toxic core of alpha-synuclein from invisible crystals. Nature 525:486–490.
7. Hoenger A (2014) High-resolution cryo-electron microscopy on macromolecular complexes and cell organelles. Protoplasma 251:417–427.
8. Schur FK, Hagen WJ, de Marco A, Briggs JA (2013) Determination of protein structure at 8.5A resolution using cryo-electron tomography and sub-tomogram averaging. J Struct Biol 184:394–400.
9. Banerjee S, Bartesaghi A, Merk A, Rao P, Bulfer SL, Yan Y, Green N, Mroczkowski B, Neitz RJ, Wipf P, Falconieri V, Deshaies RJ, Milne JL, Huryn D, Arkin M, Subramaniam S (2016) 2.3 A resolution cryo-EM structure of human p97 and mechanism of allosteric inhibition. Science 351:871–885.
10. Gonen T, Sliz P, Kistler J, Cheng Y, Walz T (2004) Aquaporin-0 membrane junctions reveal the structure of a closed water pore. Nature 429:193–197.
11. Sawaya MR, Rodriguez JA, Cascio D, Collazo M, Shi D, Reyes FE, Hattne J, Gonen T, Eisenberg DS (2106) Ab Initio structure determination from prion nanocrystals at atomic resolution by MicroED, Proc Natl Acad Sci U S A, accepted.
12. Shi D, Nannenga BL, de la Cruz MJ, Liu J, Sawtelle S, Calero G, Reyes FE, Hattne J, Gonen T (2016) The collection of MicroED data for macromolecular crystallography. Nat Protoc 11:895–904.
13. Hattne J, Reyes FE, Nannenga BL, Shi D, de la Cruz MJ, Leslie AG, Gonen T (2015) MicroED data collection and processing. Acta Crystallogr A 71:353–360.
14. Nannenga BL, Shi D, Leslie AG, Gonen T (2014) High-resolution structure determination by continuous-rotation data collection in MicroED. Nat Methods 11: 927–930.
15. Iadanza MG, Gonen T (2014) A suite of software for processing MicroED data of extremely small protein crystals. J Appl Crystallogr 47:1140–1145.
16. Arndt UW, Wonacott AJ (1977) The rotation method in crystallography: data collection from macromolecular crystals. North-Holland Publishing Company.
17. Nannenga BL, Shi D, Hattne J, Reyes FE, Gonen T (2014) Structure of catalase determined by MicroED. Elife 3:e03600.
18. Battye TG, Kontogiannis L, Johnson O, Powell HR, Leslie AG (2011) iMOSFLM: a new graphical interface for diffraction-image processing with MOSFLM. Acta Crystallogr D Biol Crystallogr 67:271–281.
19. Leslie AGW, Powell HR. Processing diffraction data with mosflm. In: Read RJ, Sussman JL, Eds. (2007) Evolving methods for macromolecular crystallography: The structural path to the understanding of the mechanism of action of CBRN agents. Dordrecht: Springer Netherlands, pp 41–51.
20. Kabsch W (2010) Xds. Acta Crystallogr D66:125–132.
21. Henderson R (1995) The potential and limitations of neutrons, electrons and X-rays for atomic resolution microscopy of unstained biological molecules. Q Rev Biophys 28:171–193.
22. Holton JM, Frankel KA (2010) The minimum crystal size needed for a complete diffraction data set. Acta Crystallogr D66:393–408.
23. Chapman HN, Fromme P, Barty A, White TA, Kirian RA, Aquila A, Hunter MS, Schulz J, DePonte DP, Weierstall U, Doak RB, Maia FR, Martin AV, Schlichting I, Lomb L, Coppola N, Shoeman RL, Epp SW, Hartmann R, Rolles D, Rudenko A, Foucar L, Kimmel N, Weidenspointner G, Holl P, Liang M, Barthelmess M, Caleman C, Boutet S, Bogan MJ, Krzywinski J, Bostedt C, Bajt S, Gumprecht L, Rudek B, Erk B, Schmidt C, Homke A, Reich C, Pietschner D, Struder L, Hauser G, Gorke H, Ullrich J, Herrmann S, Schaller G, Schopper F, Soltau H, Kuhnel KU, Messerschmidt M, Bozek JD, Hau-Riege SP, Frank M, Hampton CY, Sierra RG, Starodub D, Williams GJ, Hajdu J, Timneanu N, Seibert MM, Andreasson J, Rocker A, Jonsson O, Svenda M, Stern S, Nass K, Andritschke R, Schroter CD, Krasniqi F, Bott M, Schmidt KE, Wang X, Grotjohann I, Holton JM, Barends TR, Neutze R, Marchesini S, Fromme R, Schorb S, Rupp D, Adolph M, Gorkhover T, Andersson I, Hirsemann H, Potdevin G, Graafsma H, Nilsson B, Spence JC (2011) Femtosecond X-ray protein nanocrystallography. Nature 470:73–77.
24. Neutze R, Wouts R, van der Spoel D, Weckert E, Hajdu J (2000) Potential for biomolecular imaging with femtosecond X-ray pulses. Nature 406:752–757.
25. Zhang H, Unal H, Gati C, Han GW, Liu W, Zatsepin NA, James D, Wang D, Nelson G, Weierstall U, Sawaya MR, Xu Q, Messerschmidt M, Williams GJ, Boutet S, Yefanov OM, White TA, Wang C, Ishchenko A, Tirupula KC, Desnoyer R, Coe J, Conrad CE, Fromme P, Stevens RC, Katritch V, Karnik SS, Cherezov V (2015) Structure of the Angiotensin receptor revealed by serial femtosecond crystallography. Cell 161:833–844.

26. Johansson LC, Arnlund D, Katona G, White TA, Barty A, DePonte DP, Shoeman RL, Wickstrand C, Sharma A, Williams GJ, Aquila A, Bogan MJ, Caleman C, Davidsson J, Doak RB, Frank M, Fromme R, Galli L, Grotjohann I, Hunter MS, Kassemeyer S, Kirian RA, Kupitz C, Liang M, Lomb L, Malmerberg E, Martin AV, Messerschmidt M, Nass K, Redecke L, Seibert MM, Sjohamn J, Steinbrener J, Stellato F, Wang D, Wahlgren WY, Weierstall U, Westenhoff S, Zatsepin NA, Boutet S, Spence JC, Schlichting I, Chapman HN, Fromme P, Neutze R (2013) Structure of a photosynthetic reaction centre determined by serial femtosecond crystallography. Nat Commun 4:2911.
27. Fenalti G, Zatsepin NA, Betti C, Giguere P, Han GW, Ishchenko A, Liu W, Guillemyn K, Zhang H, James D, Wang D, Weierstall U, Spence JC, Boutet S, Messerschmidt M, Williams GJ, Gati C, Yefanov OM, White TA, Oberthuer D, Metz M, Yoon CH, Barty A, Chapman HN, Basu S, Coe J, Conrad CE, Fromme R, Fromme P, Tourwe D, Schiller PW, Roth BL, Ballet S, Katritch V, Stevens RC, Cherezov V (2015) Structural basis for bifunctional peptide recognition at human delta-opioid receptor. Nat Struct Mol Biol 22:265–268.
28. Kupitz C, Basu S, Grotjohann I, Fromme R, Zatsepin NA, Rendek KN, Hunter MS, Shoeman RL, White TA, Wang D, James D, Yang JH, Cobb DE, Reeder B, Sierra RG, Liu H, Barty A, Aquila AL, Deponte D, Kirian RA, Bari S, Bergkamp JJ, Beyerlein KR, Bogan MJ, Caleman C, Chao TC, Conrad CE, Davis KM, Fleckenstein H, Galli L, Hau-Riege SP, Kassemeyer S, Laksmono H, Liang M, Lomb L, Marchesini S, Martin AV, Messerschmidt M, Milathianaki D, Nass K, Ros A, Roy-Chowdhury S, Schmidt K, Seibert M, Steinbrener J, Stellato F, Yan L, Yoon C, Moore TA, Moore AL, Pushkar Y, Williams GJ, Boutet S, Doak RB, Weierstall U, Frank M, Chapman HN, Spence JC, Fromme P (2014) Serial time-resolved crystallography of photosystem II using a femtosecond X-ray laser. Nature 513:261–265.
29. Suga M, Akita F, Hirata K, Ueno G, Murakami H, Nakajima Y, Shimizu T, Yamashita K, Yamamoto M, Ago H, Shen JR (2015) Native structure of photosystem II at 1.95 A resolution viewed by femtosecond X-ray pulses. Nature 517:99–103.
30. Boutet S, Lomb L, Williams GJ, Barends TR, Aquila A, Doak RB, Weierstall U, DePonte DP, Steinbrener J, Shoeman RL, Messerschmidt M, Barty A, White TA, Kassemeyer S, Kirian RA, Seibert MM, Montanez PA, Kenney C, Herbst R, Hart P, Pines J, Haller G, Gruner SM, Philipp HT, Tate MW, Hromalik M, Koerner LJ, van Bakel N, Morse J, Ghonsalves W, Arnlund D, Bogan MJ, Caleman C, Fromme R, Hampton CY, Hunter MS, Johansson LC, Katona G, Kupitz C, Liang M, Martin AV, Nass K, Redecke L, Stellato F, Timneanu N, Wang D, Zatsepin NA, Schafer D, Defever J, Neutze R, Fromme P, Spence JC, Chapman HN, Schlichting I (2012) High-resolution protein structure determination by serial femtosecond crystallography. Science 337:362–364.
31. Liu W, Wacker D, Gati C, Han GW, James D, Wang D, Nelson G, Weierstall U, Katritch V, Barty A, Zatsepin NA, Li D, Messerschmidt M, Boutet S, Williams GJ, Koglin JE, Seibert MM, Wang C, Shah ST, Basu S, Fromme R, Kupitz C, Rendek KN, Grotjohann I, Fromme P, Kirian RA, Beyerlein KR, White TA, Chapman HN, Caffrey M, Spence JC, Stevens RC, Cherezov V (2013) Serial femtosecond crystallography of G protein-coupled receptors. Science 342:1521–1524.
32. Redecke L, Nass K, DePonte DP, White TA, Rehders D, Barty A, Stellato F, Liang M, Barends TR, Boutet S, Williams GJ, Messerschmidt M, Seibert MM, Aquila A, Arnlund D, Bajt S, Barth T, Bogan MJ, Caleman C, Chao TC, Doak RB, Fleckenstein H, Frank M, Fromme R, Galli L, Grotjohann I, Hunter MS, Johansson LC, Kassemeyer S, Katona G, Kirian RA, Koopmann R, Kupitz C, Lomb L, Martin AV, Mogk S, Neutze R, Shoeman RL, Steinbrener J, Timneanu N, Wang D, Weierstall U, Zatsepin NA, Spence JC, Fromme P, Schlichting I, Duszenko M, Betzel C, Chapman HN (2013) Natively inhibited Trypanosoma brucei cathepsin B structure determined by using an X-ray laser. Science 339:227–230.
33. Ayvazyan V, Baboi N, Bahr J, Balandin V, Beutner B, Brandt A, Bohnet I, Bolzmann A, Brinkmann R, Brovko OI, Carneiro JP, Casalbuoni S, Castellano M, Castro P, Catani L, Chiadroni E, Choroba S, Cianchi A, Delsim-Hashemi H, Di Pirro G, Dohlus M, Dusterer S, Edwards HT, Faatz B, Fateev AA, Feldhaus J, Flottmann K, Frisch J, Frohlich L, Garvey T, Gensch U, Golubeva N, Grabosch HJ, Grigoryan B, Grimm O, Hahn U, Han JH, Hartrott MV, Honkavaara K, Huning M, Ischebeck R, Jaeschke E, Jablonka M, Kammering R, Katalev V, Keitel B, Khodyachykh S, Kim Y, Kocharyan V, Korfer M, Kollewe M, Kostin D, Kramer D, Krassilnikov M, Kube G, Lilje L, Limberg T, Lipka D, Lohl F, Luong M, Magne C, Menzel J, Michelato P, Miltchev V, Minty M, Moller WD, Monaco L, Muller W, Nagl M, Napoly O, Nicolosi P, Nolle D, Nunez T, Oppelt A, Pagani C, Paparella R, Petersen B, Petrosyan B, Pfluger J, Piot P, Plonjes E, Poletto L, Proch D, Pugachov D, Rehlich K, Richter D, Riemann S, Ross M, Rossbach J, Sachwitz M, Saldin EL, Sandner W, Schlarb H, Schmidt B, Schmitz M, Schmuser P, Schneider JR, Schneidmiller EA, Schreiber HJ, Schreiber S, Shabunov AV, Sertore D, Setzer S, Simrock S, Sombrowski E, Staykov L, Steffen B, Stephan F, Stulle F, Sytchev KP, Thom H, Tiedtke K, Tischer M, Treusch R, Trines D, Tsakov I, Vardanyan A, Wanzenberg R, Weiland T, Weise H, Wendt M, Will I, Winter A, Wittenburg K, Yurkov MV, Zagorodnov I, Zambolin P, Zapfe K (2006) First operation of a free-electron laser generating GW power radiation at 32 nm wavelength. Eur Phys J D 37:297–303.
34. Emma P, Akre R, Arthur J, Bionta R, Bostedt C, Bozek J, Brachmann A, Bucksbaum P, Coffee R, Decker FJ, Ding Y, Dowell D, Edstrom S, Fisher A, Frisch J, Gilevich S, Hastings J, Hays G, Hering P, Huang Z, Iverson R, Loos H, Messerschmidt M, Miahnahri A, Moeller S, Nuhn HD, Pile G, Ratner D, Rzepiela J, Schultz D, Smith T, Stefan P, Tompkins H, Turner J, Welch J, White W, Wu J, Yocky G, Galayda J (2010) First lasing and operation of an angstrom-wavelength free-electron laser. Nat Photon 4:641–647.
35. Ishikawa T, Aoyagi H, Asaka T, Asano Y, Azumi N, Bizen T, Ego H, Fukami K, Fukui T, Furukawa Y, Goto S, Hanaki H, Hara T, Hasegawa T, Hatsui T, Higashiya A, Hirono T, Hosoda N, Ishii M, Inagaki T, Inubushi Y, Itoga T, Joti Y, Kago M, Kameshima T, Kimura H, Kirihara Y, Kiyomichi A, Kobayashi T, Kondo C, Kudo T, Maesaka H, Marechal XM, Masuda T, Matsubara S, Matsumoto T, Matsushita T, Matsui S, Nagasono M, Nariyama N, Ohashi H, Ohata T, Ohshima T, Ono S, Otake Y, Saji C, Sakurai T, Sato T, Sawada K, Seike T, Shirasawa K, Sugimoto T, Suzuki S, Takahashi S, Takebe H, Takeshita K, Tamasaku K, Tanaka H, Tanaka R, Tanaka T, Togashi T, Togawa K, Tokuhisa A, Tomizawa H, Tono K, Wu SK, Yabashi M,

Yamaga M, Yamashita A, Yanagida K, Zhang C, Shintake T, Kitamura H, Kumagai N. A compact X-ray free-electron laser emitting in the sub-angstrom region. Nat Photon 6:540–544.
36. Barty A, Kirian RA, Maia FRNC, Hantke M, Yoon CH, White TA, Chapman H (2014) Cheetah: software for high-throughput reduction and analysis of serial femtosecond X-ray diffraction data. J Appl Crystallogr 47: 1118–1131.
37. Foucar L, Barty A, Coppola N, Hartmann R, Holl P, Hoppe U, Kassemeyer S, Kimmel N, Kupper J, Scholz M, Techert S, White TA, Struder L, Ullrich J (2012) CASS-CFEL-ASG software suite. Comput Phys Commun 183:2207–2213.
38. White TA, Barty A, Stellato F, Holton JM, Kirian RA, Zatsepin NA, Chapman HN (2013) Crystallographic data processing for free-electron laser sources. Acta Crystallogr D69:1231–1240.
39. Hattne J, Echols N, Tran R, Kern J, Gildea RJ, Brewster AS, Alonso-Mori R, Glockner C, Hellmich J, Laksmono H, Sierra RG, Lassalle-Kaiser B, Lampe A, Han G, Gul S, DiFiore D, Milathianaki D, Fry AR, Miahnahri A, White WE, Schafer DW, Seibert MM, Koglin JE, Sokaras D, Weng TC, Sellberg J, Latimers MJ, Glatzel P, Zwart PH, Grosse-Kunstleve RW, Bogan MJ, Messerschmidt M, Williams GJ, Boutet S, Messinger J, Zouni A, Yano J, Bergmann U, Yachandra VK, Adams PD, Sauter NK (2014) Accurate macromolecular structures using minimal measurements from X-ray free-electron lasers. Nat Methods 11:545–548.
40. Arnlund D, Johansson LC, Wickstrand C, Barty A, Williams GJ, Malmerberg E, Davidsson J, Milathianaki D, DePonte DP, Shoeman RL, Wang D, James D, Katona G, Westenhoff S, White TA, Aquila A, Bari S, Berntsen P, Bogan M, van Driel TB, Doak RB, Kjaer KS, Frank M, Fromme R, Grotjohann I, Henning R, Hunter MS, Kirian RA, Kosheleva I, Kupitz C, Liang M, Martin AV, Nielsen MM, Messerschmidt M, Seibert MM, Sjohamn J, Stellato F, Weierstall U, Zatsepin NA, Spence JC, Fromme P, Schlichting I, Boutet S, Groenhof G, Chapman HN, Neutze R (2014) Visualizing a protein quake with time-resolved X-ray scattering at a free-electron laser. Nat Methods 11: 923–926.
41. Tenboer J, Basu S, Zatsepin N, Pande K, Milathianaki D, Frank M, Hunter M, Boutet S, Williams GJ, Koglin JE, Oberthuer D, Heymann M, Kupitz C, Conrad C, Coe J, Roy-Chowdhury S, Weierstall U, James D, Wang D, Grant T, Barty A, Yefanov O, Scales J, Gati C, Seuring C, Srajer V, Henning R, Schwander P, Fromme R, Ourmazd A, Moffat K, Van Thor JJ, Spence JC, Fromme P, Chapman HN, Schmidt M (2014) Time-resolved serial crystallography captures high-resolution intermediates of photoactive yellow protein. Science 346:1242–1246.
42. Barends TR, Foucar L, Ardevol A, Nass K, Aquila A, Botha S, Doak RB, Falahati K, Hartmann E, Hilpert M, Heinz M, Hoffmann MC, Kofinger J, Koglin JE, Kovacsova G, Liang M, Milathianaki D, Lemke HT, Reinstein J, Roome CM, Shoeman RL, Williams GJ, Burghardt I, Hummer G, Boutet S, Schlichting I (2015) Direct observation of ultrafast collective motions in CO myoglobin upon ligand dissociation. Science 350:445–450.
43. Nass K, Foucar L, Barends TR, Hartmann E, Botha S, Shoeman RL, Doak RB, Alonso-Mori R, Aquila A, Bajt S, Barty A, Bean R, Beyerlein KR, Bublitz M, Drachmann N, Gregersen J, Jonsson HO, Kabsch W, Kassemeyer S, Koglin JE, Krumrey M, Mattle D, Messerschmidt M, Nissen P, Reinhard L, Sitsel O, Sokaras D, Williams GJ, Hau-Riege S, Timneanu N, Caleman C, Chapman HN, Boutet S, Schlichting I (2015) Indications of radiation damage in ferredoxin microcrystals using high-intensity X-FEL beams. J Synchrotron Radiat 22:225–238.
44. Kirian RA, Wang X, Weierstall U, Schmidt KE, Spence JC, Hunter M, Fromme P, White T, Chapman HN, Holton J (2010) Femtosecond protein nanocrystallography-data analysis methods. Opt Exp 18:5713–5723.
45. Kirian RA, White TA, Holton JM, Chapman HN, Fromme P, Barty A, Lomb L, Aquila A, Maia FR, Martin AV, Fromme R, Wang X, Hunter MS, Schmidt KE, Spence JC (2011) Structure-factor analysis of femtosecond microdiffraction patterns from protein nanocrystals. Acta Crystallogr A67:131–140.
46. DePonte DP, Weierstall U, Schmidt K, Warner J, Starodub D, Spence JCH, Doak RB (2008) Gas dynamic virtual nozzle for generation of microscopic droplet streams. J Phys D 41: [PAGE #S].
47. Weierstall U, Doak RB, Spence JCH, Starodub D, Shapiro D, Kennedy P, Warner J, Hembree GG, Fromme P, Chapman HN (2007) Droplet streams for serial crystallography of proteins. Exp Fluids 44:675–689.
48. Kunnus K, Rajkovic I, Schreck S, Quevedo W, Eckert S, Beye M, Suljoti E, Weniger C, Kalus C, Grubel S, Scholz M, Nordlund D, Zhang W, Hartsock RW, Gaffney KJ, Schlotter WF, Turner JJ, Kennedy B, Hennies F, Techert S, Wernet P, Fohlisch A (2012) A setup for resonant inelastic soft x-ray scattering on liquids at free electron laser light sources. Rev Sci Instrum 83:123109.
49. Berriman J, Unwin N (1994) Analysis of transient structures by cryo-microscopy combined with rapid mixing of spray droplets. Ultramicroscopy 56:241–252.
50. Subramaniam S, Gerstein M, Oesterhelt D, Henderson R (1993) Electron diffraction analysis of structural changes in the photocycle of bacteriorhodopsin. Embo J 12:1–8.
51. Yonekura K, Kato K, Ogasawara M, Tomita M, Toyoshima C (2015) Electron crystallography of ultrathin 3D protein crystals: atomic model with charges. Proc Natl Acad Sci USA 112:3368–3373.
52. Hattne J, Shi D, de la Cruz MJ, Reyes FE, Gonen T (2016) Modeling truncated pixel values of faint reflections in MicroED imagesThis article will form part of a virtual special issue of the journal on free-electron laser software. J Appl Crystallogr 49: [PAGE #S].
53. Rossmann MG, Blow DM (1962) Detection of sub-units within crystallographic asymmetric unit. Acta Crystallogr 15:24.
54. Patterson AL (1934) A Fourier series method for the determination of the components of interatomic distances in crystals. Phys Rev 46:0372–0376.
55. Lucic V, Rigort A, Baumeister W (2013) Cryo-electron tomography: the challenge of doing structural biology in situ. J Cell Biol 202:407–419.